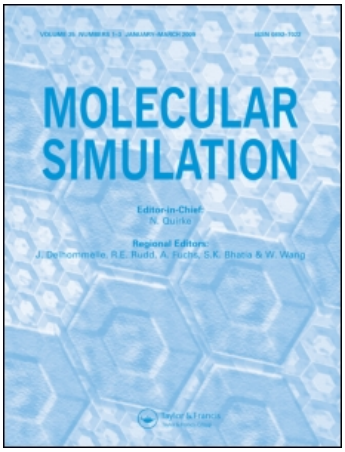


**Molecular Simulation**
Publication details, including instructions for authors and subscription information:
http://www.informaworld.com/smpp/title~content=t713644482

# Dissipative particle dynamics simulation on the meso-scale structure of diblock copolymer under cylindrical confinement

J. -B. Xu[a]; H. Wu[a]; D. -Y. Lu[b]; X. -F. He[b]; Y. -H. Zhao[b]; H. Wen[b]
[a] Graduate School of the Chinese Academy of Sciences, Beijing, P.R. China [b] Multi-phase Reaction Laboratory, Institute of Process Engineering, Chinese Academy of Sciences, Beijing, P.R. China

**To cite this Article** Xu, J. -B. , Wu, H. , Lu, D. -Y. , He, X. -F. , Zhao, Y. -H. and Wen, H.(2006) 'Dissipative particle dynamics simulation on the meso-scale structure of diblock copolymer under cylindrical confinement', Molecular Simulation, 32: 5, 357 — 362
**To link to this Article: DOI:** 10.1080/08927020600702022
**URL:** http://dx.doi.org/10.1080/08927020600702022

*Molecular Simulation*, Vol. 32, No. 5, 30 April 2006, 357–362

Taylor & Francis
Taylor & Francis Group

# Dissipative particle dynamics simulation on the meso-scale structure of diblock copolymer under cylindrical confinement

J.-B. XU†‡, H. WU†‡, D.-Y. LU†, X.-F. HE†, Y.-H. ZHAO† and H. WEN†*

†Multi-phase Reaction Laboratory, Institute of Process Engineering, Chinese Academy of Sciences, No. 1, 2nd North Lane, Zhong-Guan-Cun, Beijing 100080, P.R. China
‡Graduate School of the Chinese Academy of Sciences, Beijing 100049, P.R. China

*(Received January 2006; in final form March 2006)*

The meso-scale structure of symmetric diblock copolymer under cylindrical confinement is studied by dissipative particle dynamics (DPD). The simulation results show that coiled cylindrical geometry is favored in the presence of larger cylinder radius ($R/L_0 > \sim 1.5$), and the number of rings depends on the cylinder radius. Because of the cylinder wall's selectivity, each block can form the central core, but only the preferential block forms the outmost layer. An approximately linear relationship exists between structure transition point, which is approximately in proportion to the 3/5 exponential of chain length of copolymer and number of layers. As the cylinder radius is decreased, a helical morphology is found. Lamellae parallel to the underside of the cylinder appear when the cylinder radius is made smaller ($R/L_0 < \sim 1.1$).

*Keywords*: Block copolymer; Dissipative particle dynamics; Solid boundary condition; Meso-scale simulation; Confinement



## 1. Introduction

In the past decades, the morphologies and micro-phase transitions of block copolymer thin films confined by impenetrable hard walls have been extensively investigated because of their potential applications in nanofabrication. For the symmetric diblock copolymer films, the structural periodicity and the orientation of lamellae have been examined in a number of publications [1–21]. The change of the lamellar pattern in thin films of diblock copolymers confined between two parallel hard walls is studied by dissipative particle dynamics (DPD) in our pervious work [22]. For symmetric diblock copolymer film confined between two flat surfaces, the preferential segregation of one of the blocks to the interfaces forces an orientation of the micro domains parallel to the walls, resulting in a multi-lamellar film structure. The lamellae will orient normal to the surface, when the energy required to stretch or compress the copolymer chains is greater than the total interfacial energies. In contrast to the diblock copolymer film, only a few works performed on the diblock copolymers confined by cylinder to our knowledge. He *et al.* [23] and Sevink *et al.* [24] recently performed Monte Carlo simulations and self-consistent theoretical calculations, respectively. For symmetric diblock copolymer confined within cylindrical pores, if the cylinder is preferential to one block, the so-called "concentric barrel" or "dartboard" morphology was predicted. Xiang *et al.* [25–28] investigated the two-dimensional confinement of symmetric diblock copolymers of styrene and butadiene using nano-scopic cylindrical pores in alumina membranes. A multiple set of concentric cylinders is found when the pore diameter is large in comparison to the equilibrium period. As the pore diameter decreases, a helical morphology appears. Wu *et al.* [29] systematically studied the confined assembly of silica-copolymer composite meso-structures within cylinders of varying diameters. Single- and double-helical geometries were found.

In this paper, DPD [30] simulations are performed to examine the meso-structural morphologies of symmetric diblock copolymers confined by cylindrical wall and the micro-phase transitions with increasing or decreasing the radius of cylindrical wall. Moreover, the simulation results including the end-to-end distance of copolymer chains, the character of the meso-structure are also investigated extensively.

*Corresponding author. Tel.: +86-10-62626704. Email: hwen@home.ipe.ac.cn

*Molecular Simulation*
ISSN 0892-7022 print/ISSN 1029-0435 online © 2006 Taylor & Francis
http://www.tandf.co.uk/journals
DOI: 10.1080/08927020600702022

## 2. Dissipative particle dynamics

The DPD method describes a fluid system by dividing it up in small interacting fluid packages. Each package is represented by a DPD bead. The evolution of the positions ($\mathbf{r}_{ij}$) and impulses ($\mathbf{v}_{ij}$) of all interacting beads over time is governed by the Newtonian second law of motion.

$$\frac{\partial \mathbf{r}_i}{\partial t} = \mathbf{v}_i, \quad m_i \frac{\partial \mathbf{v}_i}{\partial t} = \mathbf{f}_i \tag{1}$$

The equations of motion are solved using the modified velocity-Verlet algorithm presented by Groot and Warren [31]. The total force acting on a bead is composed of three pairwise additive forces, conservative ($\mathbf{F}_{ij}^{\mathrm{C}}$), dissipative ($\mathbf{F}_{ij}^{\mathrm{D}}$) and random ($\mathbf{F}_{ij}^{\mathrm{R}}$).

$$\mathbf{f}_i = \sum_{j \neq i} \left( \mathbf{F}_{ij}^{\mathrm{C}} + \mathbf{F}_{ij}^{\mathrm{D}} + \mathbf{F}_{ij}^{\mathrm{R}} \right) \tag{2}$$

Beads interact only with beads that are within a certain cut-off radius $r_{\mathrm{c}}$. If $r_{\mathrm{c}} = 1$, then

$$\mathbf{F}_{ij}^{\mathrm{C}} = \begin{cases} a_{ij}(1 - r_{ij})\mathbf{r}_{ij} & r_{ij} < 1 \\ 0 & r_{ij} > 1 \end{cases} \tag{3}$$

$$\mathbf{F}_{ij}^{\mathrm{D}} = \begin{cases} -\gamma \omega^{\mathrm{D}}(r_{ij})(\mathbf{r}_{ij} \cdot \mathbf{v}_{ij})\mathbf{r}_{ij} & r_{ij} < 1 \\ 0 & r_{ij} > 1 \end{cases} \tag{4}$$

$$\mathbf{F}_{ij}^{\mathrm{R}} = \begin{cases} \sigma \omega^{\mathrm{R}}(r_{ij}) \xi_{ij} \mathbf{r}_{ij} & r_{ij} < 1 \\ 0 & r_{ij} > 1 \end{cases} \tag{5}$$

Here, $\xi_{ij}$ is a random number drawn from a uniform distribution with zero mean, $\omega(r_{ij})$ is the weight function, $\gamma$ is a friction factor and $\sigma$ defines the fluctuation amplitude.

Español and Warren [32] have shown that the system relaxes to a Gibbs–Boltzmann equilibrium distribution when the correct thermostat is applied. They proved that this hold true if the random and dissipative forces are balanced and related to the system temperature according the fluctuation–dissipation theorem

$$\omega^{\mathrm{D}}(r) = [\omega^{\mathrm{R}}(r)]^2 \tag{6}$$

$$\sigma^2 = 2\gamma k_{\mathrm{B}} T \tag{7}$$

Here, $k_{\mathrm{B}}$ is the Boltzmann constant. The weight functions, tending to zero for $r_{ij} \rightarrow 1$, can have the following simple form.

$$\omega^{\mathrm{D}}(r) = [\omega^{\mathrm{R}}(r)]^2 = (1 - r)^2 \quad r \leq 1 \tag{8}$$

A simple velocity-Verlet like algorithm described by Groot and Warren [31] is used to integrate the equations of motion. The simulations in this paper are performed with $k_{\mathrm{B}}T = 1.0$, $\sigma = 3.0$, $\rho = 3.0$ and $\Delta t = 0.03$.

## 3. Simulation details

### 3.1 Boundary method for cylindrical solid wall

Until now, two boundary methods have been considered in the treatment of boundary conditions for cylindrical solid wall in DPD simulations. Darias *et al.* [33] constructed curved walls by means of a bounce-back reflection alone, without particles physically constructing it. The deficiency of repulsive force results in an accumulation of particles at the wall. Visser *et al.* [34] constructed curved walls by folding the mirror image of the system around the curved boundary. In order to compensate for the alterations of the particle density inside that image caused by folding, the positions of the particles across the wall boundary for every interaction with a system particle are rescaled. However, this boundary method is not fit for the depiction of the walls' effect on the system.

In this paper, frozen beads are used to construct the cylindrical wall and the density of the wall particle is defined as the same as that of the diblock copolymer melts. The frozen beads interact as normal fluid beads, but the positions of which are fixed and the velocities are set to be zero. The wall particles are shifted outward by half inter-particle distance away from the boundary, which is $\rho^{-1/3}/2$, to weaken the density distortion near the wall [35]. The thickness of the wall is set to be $1 - \rho^{-1/3}/2$, where 1 is the cutoff radius in DPD simulation. The length of the cylindrical wall is set to be 20. Periodic boundary condition is used in the axis direction of the cylindrical wall. To guarantee the wall's impenetrability, the reflecting boundary condition is used.

### 3.2 Model and details of the simulation

The symmetric diblock copolymer is composed of beads A and B, expressed as A$m$B$m$, where $m$ is the number of beads in each block. The inner radius of the cylindrical wall $R$ varies from 2 to 21, and the length of copolymer chain $N$ is 8, 12, 16, 20, 24, 32 and 36. Thus, the number of copolymer and wall particles can be calculated by $20\pi R^2/3N$ and $20\pi[(R+1)^2 - (R+\rho^{-1/3})]^2/3N$, respectively. Repulsive parameters $a_{ij}$ between beads of wall and those in copolymer chain are used to incarnate the selectivity of the wall, as shown in table 1. Every system runs by 60,000 time steps.

The variety of system properties is monitored, including the end-to-end distance of copolymer chain, and the density profiles of beads A and B are those used to determine the number and the thickness of cylindrical lamellae.

Table 1. The repulsive parameters ($a_{ij}$) between beads A, B and walls.

| *Beads* | *A* | *B* | *Walls* |
|---|---|---|---|
| A | 25 | 35 | 30 |
| B | 35 | 25 | 40 |
| Walls | 30 | 40 | – |

## 4. Results and discussion

### 4.1 Morphology of meso-structure under cylindrical confinement

As discussed in our pervious work [22], the micro-phase of symmetric diblock copolymer films confined between two hard parallel walls will separate into lamellae at equilibrium. However, a curvature is forced on the lamellar morphology when the diblock copolymers are under cylindrical confinement, as presented in figure 1 for the simulations on the micro-phase transition of diblock copolymer A8B8. Table 2 shows the relationships between $L_0$, $N$, $R_1$ and $R_2$. Here, $L_0$, called as natural period of diblock copolymer, is the equilibrium lamella thickness of bulk lamella copolymers without any confinement. $L_0$ is proportional to $N^{2/3}$, this relationship is consistent with theoretical findings [6]. $R_1$ and $R_2$ are respectively the radius where the structural transitions from lamellar to helical morphology, and from helical to concentric cylindrical morphology take place.

Figure 1 and table 2 indicate that the bulk lamellae-forming copolymer will separate into concentric cylindrical geometry when $R/L_0$ is larger than $\sim 1.5$, which is nearly the same as the results reported by Xiang *et al.* [25–27]. The outer lamella of concentric cylinders is always composed by the blocks of beads A (black balls in figure 1) in diblock copolymer, which are more preferential to the cylindrical wall. However, either blocks of beads A or B can form the central core, depending on the radius of cylindrical wall. As a result, the number of concentric cylindrical lamellae will increase periodically as the radius of cylindrical wall increased. Unlike the micro-phase transition of diblock copolymer confined between two hard parallel walls, where irregular transition morphology will appear when the micro-phase transferring from $n$ to $n+1$ lamellae [22], no irregularity in micro-phase transition is found when the number of concentric cylindrical lamellae increased. A helical morphology as shown in figure 1(B) is found as the cylinder radius decreases, which is also found by Xiang *et al.* [28]. When the radius decreases further, e.g. when $R/L_0$ is lower than $\sim 1.1$, lamellae parallel to the underside of the cylindrical wall appear as shown in figure 1(A).

Table 2. Relationships between $L_0$, $N$ and the structure transitions radius.

| $N$ | $L_0$ | $0.525N^{2/3}$ | $R_1$ | $R_1/L_0$ | $R_2$ | $R_1/L_0$ |
|---|---|---|---|---|---|---|
| 8 | 2.1 | 2.1 | 2.5 | 1.190 | 3 | 1.428 |
| 12 | 2.8 | 2.752 | 3 | 1.071 | 4.5 | 1.607 |
| 16 | 3.35 | 3.336 | 3.5 | 1.045 | 5.25 | 1.567 |
| 20 | 3.9 | 3.868 | 4.25 | 1.090 | 6 | 1.538 |
| 24 | 4.35 | 4.368 | 4.75 | 1.092 | 6.5 | 1.494 |
| 32 | 5.3 | 5.292 | 6 | 1.132 | 8 | 1.509 |
| 36 | 5.8 | 5.724 | 6.25 | 1.078 | 8.75 | 1.509 |

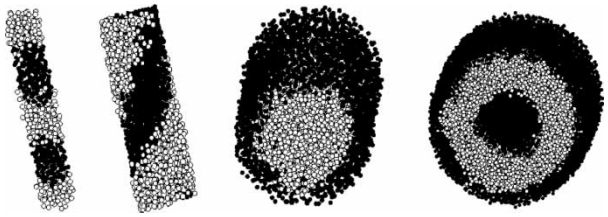


Figure 1. Micro-phase transitions of symmetric diblock copolymer A8B8 at $R/L_0 = 0.5 \sim 5.0$.

### 4.2 Thickness of concentric cylindrical lamellae

Figure 1 states that the symmetric diblock copolymer under cylindrical confinement will present a meso-structure of concentric cylindrical lamellae, when $R/L_0$ is larger than $\sim 1.5$. The number of concentric cylindrical lamellae undergoes a series of discrete increase from $n$ to $n+1$, and the thickness of each lamella will increase at a given number of lamellae, as increasing the radius of cylindrical wall. Figure 2 presents an example of radial density profiles of beads A and B, which can be used to determine the lamellar thickness from the cross point of density profiles. A slight density distortion can be found nearby the wall. However, in the middle of the cylinder the density has the desired level.

Figure 3 presents an approximately linear relationship exists between the lamellar thickness and the radius of cylindrical wall for the A/B and A/B/A concentric cylindrical structures of symmetric diblock copolymer A8B8. The slope of the linear relationship for inner lamella is larger than that for outer lamella, which indicates that the thickness increasing on inner lamella is more evident than that on outer lamella. Furthermore, the larger the number of concentric cylindrical lamellae, the less significant is the perturbation of the lamellar thickness. Same situation can also be observed in the system of different length of copolymer chain. Table 3 presents the slopes of the linear relationships for the

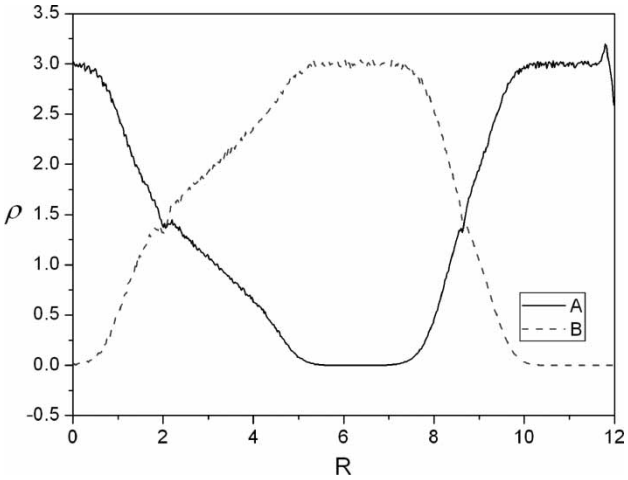


Figure 2. An example of radial density profiles of beads A and B.

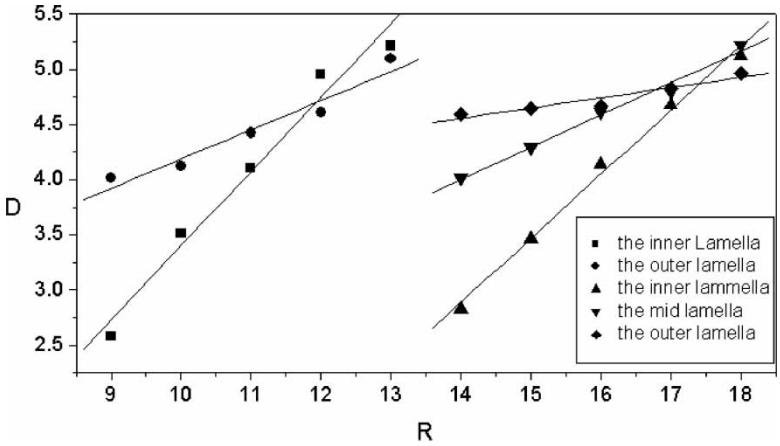


Figure 3. Relationship between the lamellar thickness and the radius of cylindrical wall for diblock copolymer A8B8.

Table 3. Slopes of the linear relationships on lamellar thickness for the A/B/A concentric cylindrical structures of symmetric diblock copolymers with different chain length.

| | *Slopes for lamellar thickness* | | |
|---|---|---|---|
| *Diblock copolymer* | *Inner lamella* | *Mid lamella* | *Outer lamella* |
| A8B8 | 0.6706 | 0.2652 | 0.0642 |
| A10B10 | 0.6133 | 0.3009 | 0.0859 |
| A12B12 | 0.5832 | 0.3192 | 0.0976 |
| A16B16 | 0.6178 | 0.2948 | 0.0875 |
| A18B18 | 0.6130 | 0.3045 | 0.0825 |
| Average | 0.6196 | 0.2969 | 0.0835 |



A/B/A concentric cylindrical structures of diblock copolymers of A8B8, A10B10, A12B12, A16B16 and A18B18. Even quite different length of copolymer chain appears in Table 3, the slopes of the linear relationships for a given lamella are almost constant. Moreover, the inner lamella has larger slope, in other words, the larger perturbation of lamellar thickness is observed towards the center of cylinder, which is the same as the results presented by Xiang *et al.* [27].

### *4.3 End-to-end distance of diblock copolymers*

Free energy of the simulation system can be composed from three contributions, the entropic penalty for deforming the chains from their disordered state conformation, the interfacial energy from segregating the blocks of beads A and B, and the surface interaction between the simulation system and the walls. When the repulsive parameters and the length of copolymer chain are fixed, the radius of cylindrical wall becomes the only factor affecting the morphology of the simulation system. The end-to-end distance of diblock copolymer molecules can be an important parameter exhibiting the changes of meso-structure, as increasing or decreasing the radius of cylindrical wall.

Figure 4 shows that the end-to-end distance of diblock copolymer A4B4 will fluctuate periodically as increasing the radius of cylindrical wall. The period of fluctuation is synchronous with micro-phase transition, and the amplitude of fluctuation becomes less and less corresponding to the change of lamellar thickness. Moreover, the average value of end-to-end distance of each period is increased gradually, which can also be related to the perturbation of the lamellar thickness as discussed in former section. The end-to-end distance can be calculated by the following formula, when the end-to-end distance is supposed to be close to the layer thickness.

$$r \approx \sum_{i=1}^{n} D_i P_i \tag{9}$$

Here, $D_i$ is the thickness of the $i$th lamella, $P_i$ is the proportion of the copolymer beads in the $i$th lamella. As discussed in the former section, the change of the inner lamellar thickness is more significant in one period, while the proportion of the polymer beads in inner lamella decreases quadratic with increasing the radius of the cylindrical wall. That is, the perturbation of the end-to-end distance is mostly caused by the thickness change of the inner lamella. However, the effect of the inner lamella is decreased quadratic following the proportion's change with the increase of lamellar number. As a result, the average end-to-end distance increases gradually.

### *4.4 Structure transition point*

In the case of $R/L_0 > \sim 1.5$, where the morphology of concentric cylinders is found and the number of concentric cylindrical lamellae increases periodically increasing the radius of cylindrical walls, the structure transition point can be defined in this paper as such a radius of cylindrical walls where the micro-phase transitions take place. Figure 5 shows that a linear relationship exists between the structure transition point and the number of lamellae for diblock copolymer A4B4, and the transition period is slightly larger than the natural period of diblock copolymer. The same relationship exists in the micro-phase transitions of diblock copolymer films confined between two hard parallel walls [22].

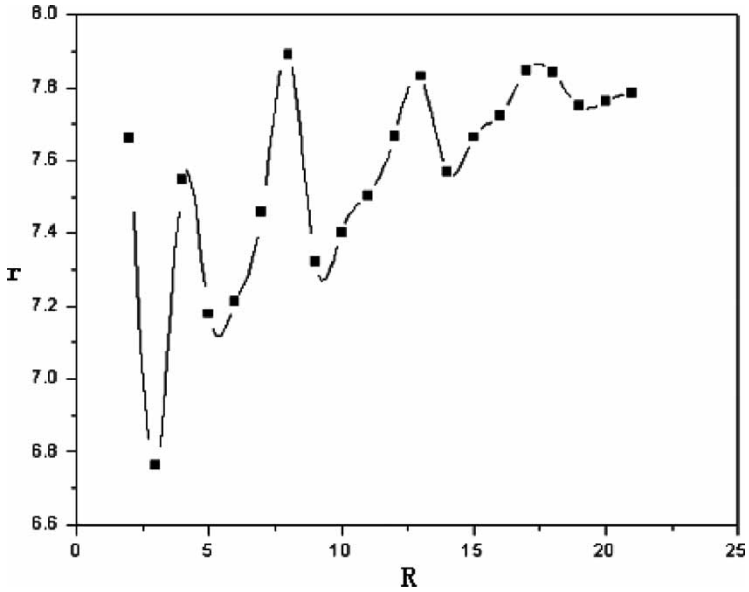


Figure 4. End-to-end distance of diblock copolymer A4B4 as function of the radius of cylindrical wall.



The structure transition point is also increased as increasing the length of copolymer chain. Figure 6 presents the relationship between the structure transition point and the length of copolymer chain $N$, where logarithmic coordinates are used which indicates the relationship of $R \propto N^x$ exists. For the relationships presented in figure 5 for the 2- and 3-lamellae concentric cylinders of different length of copolymer chain, the values of exponent $x$ are 0.6186 and 0.5833, respectively, which is close to 2/3 in the exponential relation between $L_0$ and $N$.

## 5. Conclusions

DPD is applied in the meso-scale structure of symmetric diblock copolymer under cylindrical confinement. The simulation results reveal that the bulk lamella-forming copolymer separated into coiled cylindrical geometry when the ratio of cylinder radius to the natural period of the copolymer is larger than $\sim 1.5$. The number of rings increases periodically with the increase in the cylinder radius. The thickness of every ring increased with the increase of cylinder radius in one period of given number of rings and the perturbation of the inner rings' thickness is more significant than the outer one. Moreover, the larger the ring number, the less significant is the perturbation of the ring thickness. The end-to-end distance of the diblock copolymers fluctuates periodically that is homologous with the transition of $n-n+1$ ring, and the fluctuate range becomes less and less with the increase of the cylinder radius. The average end-to-end distance of every period is increased gradually because of the uneven change of the perturbation of ring thickness in one period. The structure transition point is linear with the ring numbers, and is approximately in proportion to the 3/5 exponential of

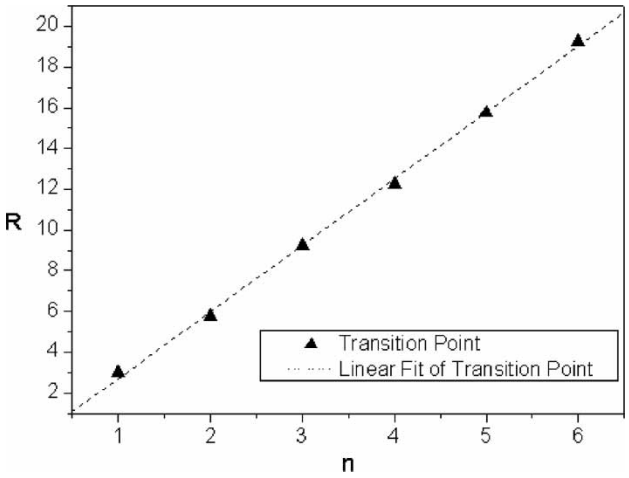


Figure 5. Relationship between the structure transition point and the number of concentric cylindrical lamellae for diblock copolymer A4B4.

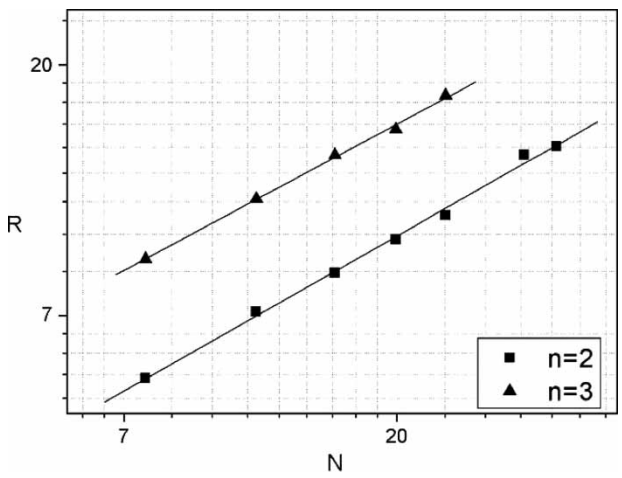


Figure 6. The relationship between the polymer length $N$ and the structure transition point.

chain length of copolymer. As the cylinder radius decreases, a helical morphology is found, then lamellae parallel to the underside of the cylinder appear when the ratio of cylinder radius to the natural period of the polymer is reduced to $\sim 1.1$.

## Acknowledgements

The authors are grateful to the National Natural Science Foundation of China for the financial support by the project 20221603 and 20273075.

## References

[1] P. Lambooy, T.P. Russell, G.J. Kellogg, A.M. Mayes, P.D. Gallagher, S.K. Satija. Observed frustration in confined block-copolymers. *Phys. Rev. Lett.*, **72**, 2899 (1994).
[2] T.P. Russell, P. Lambooy, G.J. Kellogg, A.M. Mayes. Diblock copolymers under confinement. *Physica B*, **213**, 22 (1995).
[3] N. Koneripalli, N. Singh, R. Levicky, F.S. Bates, P.D. Gallagher, S.K. Satija. Confined block copolymer thin films. *Macromolecules*, **28**, 2897 (1995).
[4] Q. Wang, Q. Yan, P.F. Nealey, J.J. de Pablo. Monte Carlo simulations of diblock copolymer thin films confined between two homogeneous surfaces. *J. Chem. Phys.*, **112**, 450 (2000).
[5] K.R. Shull. Mean-field theory of block copolymers: bulk melts, surfaces, and thin films. *Macromolecules*, **25**, 2122 (1992).
[6] M.S. Turner. Equilibrium properties of a diblock copolymer lamellar phase confined between flat plates. *Phys. Rev. Lett.*, **69**, 1788 (1992).
[7] D.G. Walton, G.J. Kellogg, A.M. Mayes, P. Lambooy, T.P. Russell. A free energy model for confined diblock copolymers. *Macromolecules*, **27**, 6225 (1994).
[8] G. Brown, A. Chakrabarti. Ordering of block copolymer melts in confined geometry. *J. Chem. Phys.*, **102**, 1440 (1995).
[9] G.T. Pickett, A.C. Balazs. Equilibrium orientation of confined diblock copolymer films. *Macromolecules*, **30**, 3097 (1997).
[10] M.W. Masten. Thin films of block copolymer. *J. Chem. Phys.*, **106**, 7781 (1997).
[11] G.J. Kellogg, D.G. Walton, A.M. Mayes, P. Lambooy, T.P. Russell, P.D. Gallagher, S.K. Satija. Observed surface energy effects in confined diblock copolymers. *Phys. Rev. Lett.*, **76**, 2503 (1996).
[12] M. Kikuchi, K. Binder. Microphase separation in thin films of the symmetric diblock-copolymer melt. *J. Chem. Phys.*, **101**, 3367 (1994).
[13] T. Geisinger, M. Muller, K. Binder. Symmetric diblock copolymers in thin films. I. Phase stability in self-consistent field calculations and Monte Carlo simulations. *J. Chem. Phys.*, **111**, 5241 (1999).
[14] Q. Wang, S.K. Nath, M.D. Graham, P.F. Nealey, J.J. de Pablo. Symmetric diblock copolymer thin films confined between homogeneous and patterned surfaces: simulations and theory. *J. Chem. Phys.*, **112**, 9996 (2000).
[15] G.G. Pereia, D.R.M. Williams. Thin films of perpendicularly oriented diblock copolymers: lamellar distortions driven by surface-diblock interfacial tensions. *Macromolecules*, **32**, 1661 (1999).
[16] G.G. Pereira, D.R.M. Williams. Lamellar interface distortions of thin, commensurately aligned diblock copolymer films on patterned surfaces. *Langmuir*, **15**, 2125 (1999).
[17] G.G. Pereira, D.R.M. Williams. Surface crinkling of strained diblock copolymer smectic thin films on striped substrates. *Europhys. Lett.*, **44**, 302 (1998).
[18] G.G. Pereira, D.R.M. Williams. Diblock copolymer thin films on heterogeneous striped surfaces: commensurate, incommensurate and inverted lamellae. *Phys. Rev. Lett.*, **80**, 2849 (1998).
[19] G.G. Pereira, D.R.M. Williams. Equilibrium properties of diblock copolymer thin films on a heterogeneous, striped surface. *Macromolecules*, **31**, 5904 (1998).
[20] G.G. Pereira, D.R.M. Williams. Diblock copolymer thin film melts on striped, heterogeneous surfaces: parallel, perpendicular and mixed lamellar morphologies. *Macromolecules*, **32**, 758 (1999).
[21] H.D. Zhang, J.W. Zhang, Y.L. Yang, X.D. Zhou. Microphase separation of diblock copolymer induced by directional quenching. *J. Chem. Phys.*, **106**, 784 (1997).
[22] J.B. Xu, H. Wu, D.Y. Lu, X.F. He, H. Wen. Dissipative particle dynamics simulation on the meso-scale structure of diblock copolymer film. *Acta Phys.-Chim.*, **22**, 16 (2006).
[23] X.H. He, M. Song, H.J. Liang, C.Y. Pan. Self-assembly of the symmetric diblock copolymer in a confined state: Monte Carlo simulation. *J. Chem. Phys.*, **114**, 10510 (2001).
[24] G.J.A. Sevink, A.V. Zvelindovsky, J.G.E.M. Fraaije, H.P. Huinink. Morphology of symmetric block copolymer in a cylindrical pore. *J. Chem. Phys.*, **115**, 8226 (2001).
[25] H. Xiang, K. Shin, T. Kim, S.I. Moon, T.J. McCarthy, T.P. Russell. Block copolymers under cylindrical confinement. *Macromolecules*, **37**, 5660 (2004).
[26] K. Shin, H. Xiang, S.I. Moon, T. Kim, T.J. McCarthy, T.P. Russell. Curving and frustrating flatland. *Science*, **306**, 76 (2004).
[27] H. Xiang, K. Shin, T. Kim, S.I. Moon, T.J. McCarthy, T.P. Russell. The influence of confinement and curvature on the morphology of block copolymers. *J. Polym. Sci: Part B: Polym. Phys.*, **43**, 3377 (2005).
[28] H. Xiang, K. Shin, T. Kim, S.I. Moon, T.J. McCarthy, T.P. Russell. From cylinders to helices upon confinement. *Macromolecules*, **38**, 1055 (2005).
[29] Y.Y. Wu, G.S. Cheng, K. Katsov, S.W. Sides, J.F. Wang, J. Tang, G.H. Fredrickson, M. Moskovitis, G.D. Stucky. Composite mesostructures by nano-confinement. *Nat. Mater.*, **3**, 816 (2004).
[30] P.J. Hoogerbrugge, J.M.V.A Koelman. Simulating microscopic hydrodynamics phenomena with dissipative particle dynamics. *Europhys. Lett.*, **19**, 155 (1992).
[31] R.D. Groot, P.B. Warren. Dissipative particle dynamics: bridging the gap between atomistic and mesoscopic simulation. *J. Chem. Phys.*, **107**, 4423 (1997).
[32] P. Español, P. Warren. Hydrodynamics from dissipative particle dynamics. *Phys. Rev. E*, **52**, 1734 (1995).
[33] J.R. Darias, M. Quiroga, E. Medina, P.J. Colmenares, R. Paredes V. Simulation of suspensions in constricted geometries by dissipative particle dynamics. *Mol. Simul.*, **29**, 443 (2003).
[34] D.C. Visser, H.C.J. Hoefsloot, P.D. Iedema. Comprehensive boundary method for solid walls in dissipative particle dynamics. *J. Comput. Phys.*, **205**, 626 (2005).
[35] I.V. Pivkin, G.E. Karniadakis, A. new. method to impose no-slip boundary conditions in dissipative particle dynamics. *J. Comput. Phys.*, **207**, 114 (2005).